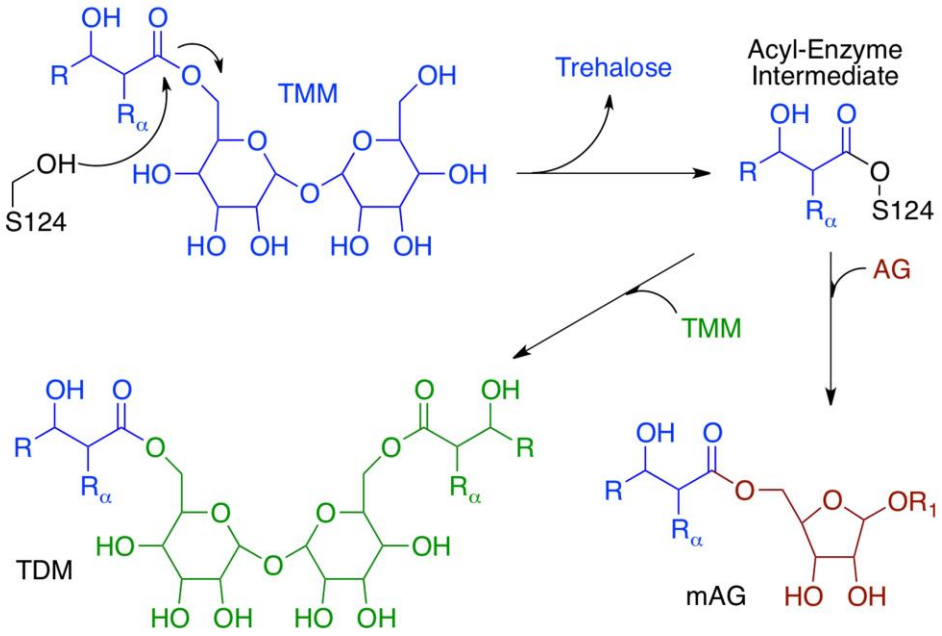

Supplementary Figure S1. Reactions catalyzed by the Ag85 complex. Reaction of TMM with Ag85 forms an acyl-enzyme intermediate. Depending on the identity of the enzyme, this intermediate then transfers the mycolyl group to either another TMM molecule or the mAG.

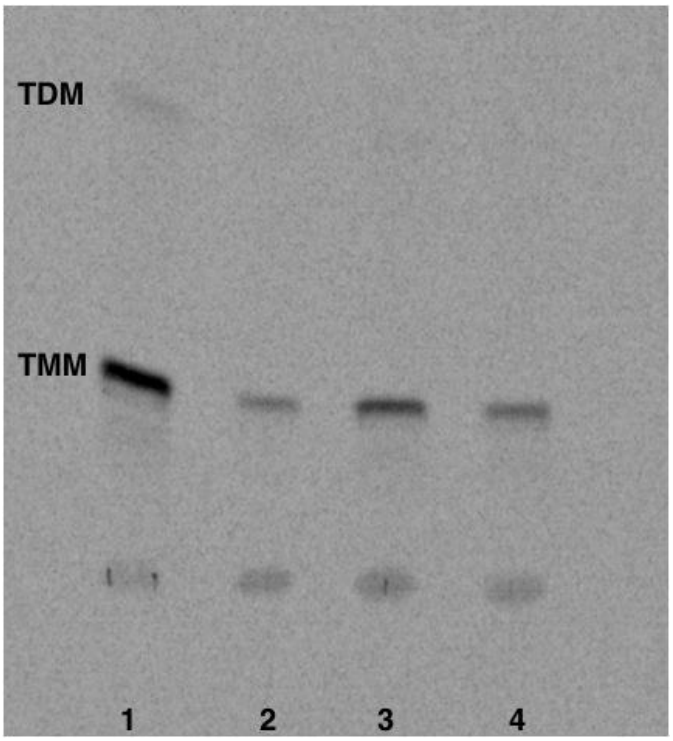

Supplementary Figure S2. Radiometric mycolyltransferase assays measuring the activity of the Ag85A and B proteins in the presence of TMM, [U-^{14}C] trehalose and 0 or 10 μM EBS. The products of the reaction were analyzed by TLC (chloroform:methanol:water; 20:4:0.5, v/v) and revealed by autoradiography. The same volume of sample was loaded in each lane. Lanes 1 and 3 correspond to untreated Ag85A and B, respectively, while lanes 2 and 4 correspond to Ag85A or B incubated with 10 μM EBS. The amount of radioactivity incorporated in the products of interest was semiquantified using a Phosphorimager. For Ag85A, TDM production was reduced 91.6% in presence of EBS while TMM production decreased by 82.4%. For Ag85B, TDM synthesis is completely abolished whereas TMM production is reduced 39.2% compared to the control.

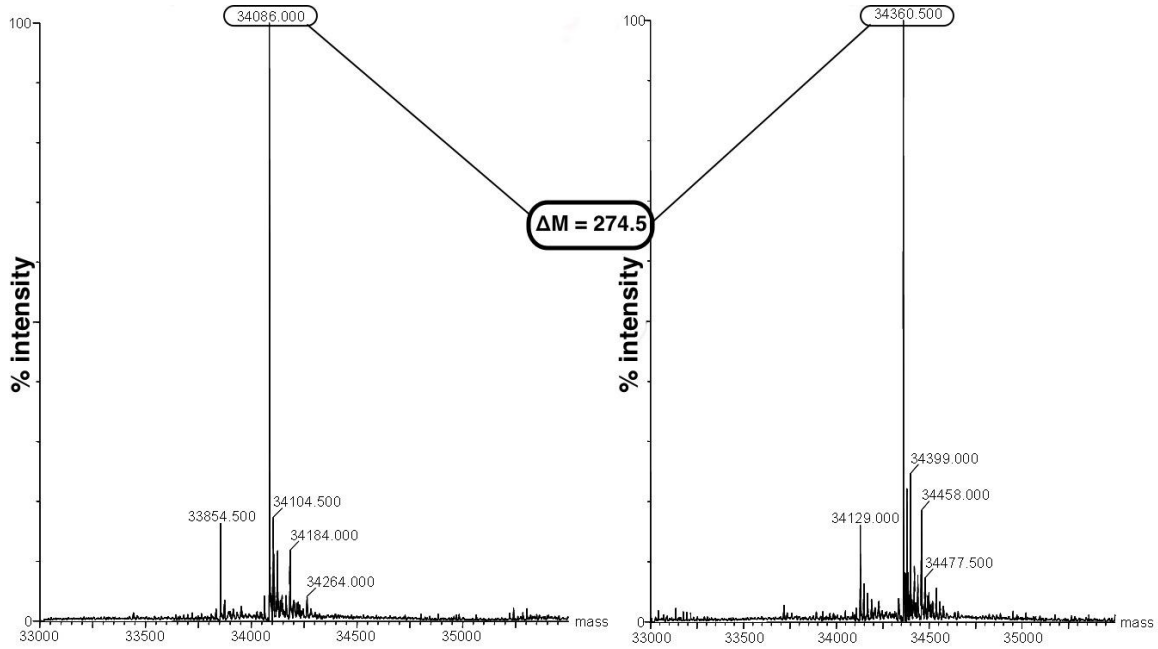

Supplementary Figure S3. Intact mass of Ag85A with and without EBS. On the left, the deconvoluted ESI mass spectrum showing the intact mass of Ag85A. On the right, the deconvoluted ESI mass spectrum showing the intact mass of an Ag85A-EBS covalent complex.

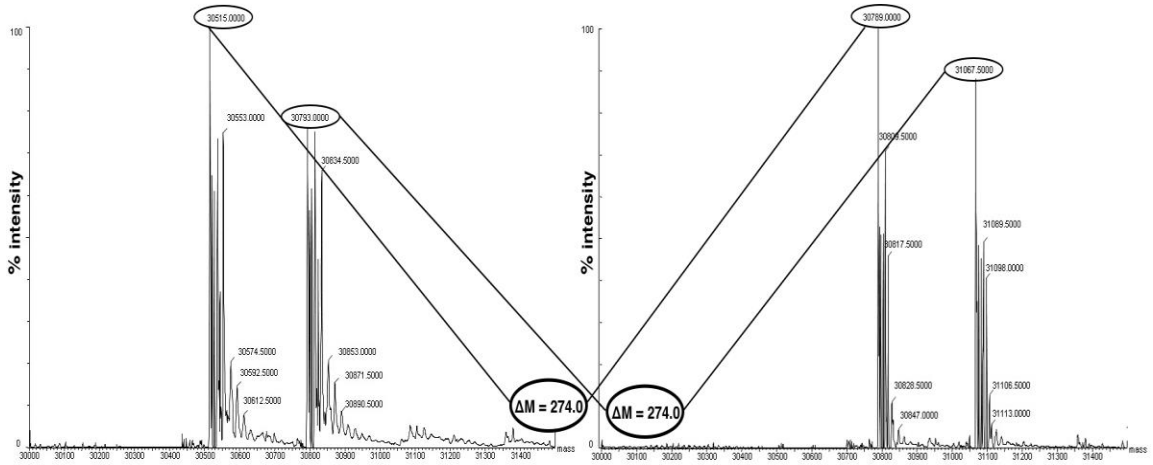

Supplementary Figure S4. Intact mass of Ag85B with and without EBS. On the left, the deconvoluted ESI mass spectrum showing the intact mass of Ag85B. On the right, the deconvoluted ESI mass spectrum showing the intact mass of an Ag85B-EBS covalent complex. Two different intact masses of Ag85B were observed on each deconvoluted ESI mass spectrum. This is likely due to proteolytic degradation of one of the enzyme termini.

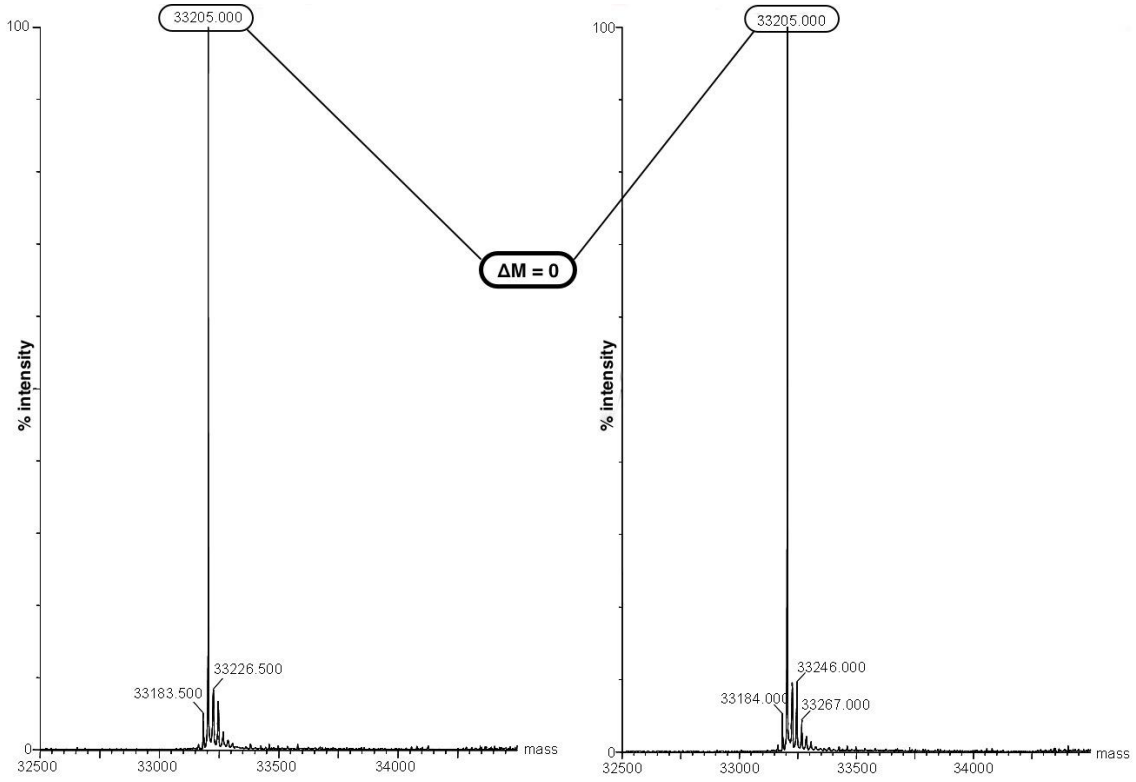

Supplementary Figure S5. Intact mass of Ag85C-C209S with and without EBS. On the left, the deconvoluted ESI mass spectrum showing the intact mass of Ag85C-C209S. On the right, the deconvoluted ESI mass spectrum showing the intact mass of Ag85C-C209S reacted with EBS. No difference in mass is observed between the two samples, showing that EBS does not covalently modify Ag85C-C209S.

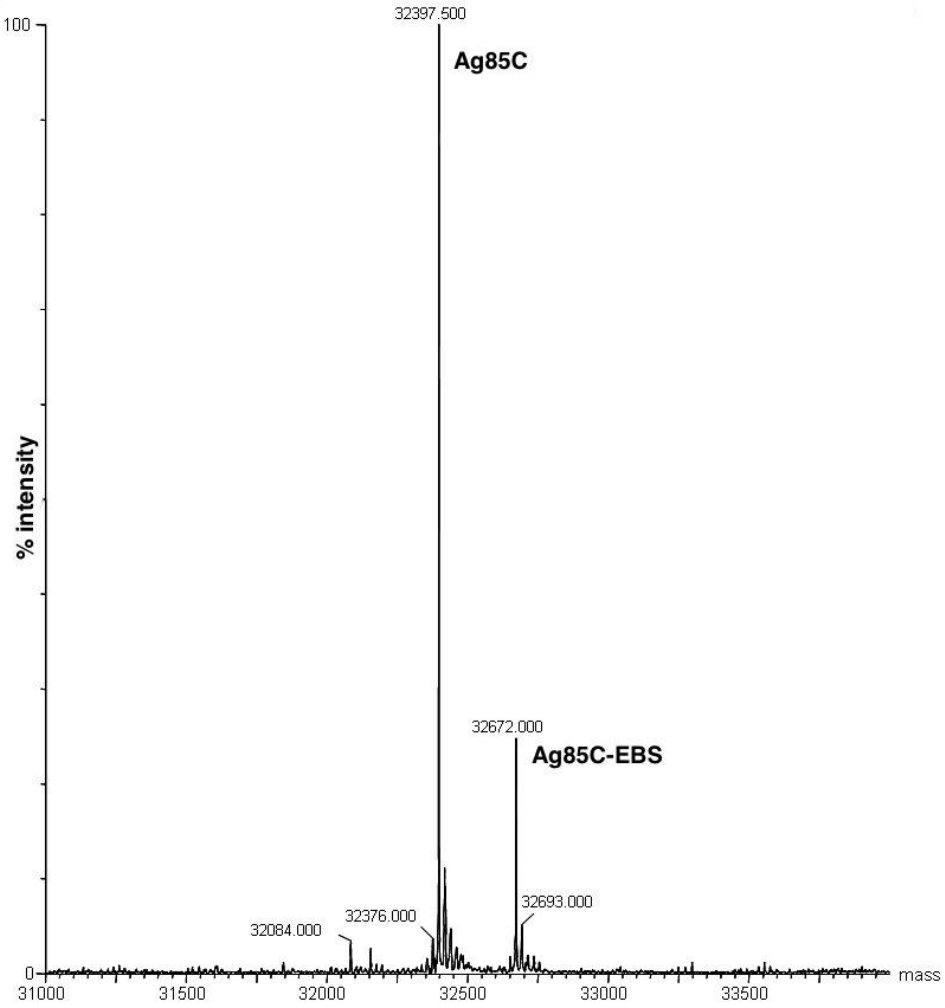

Supplementary Figure S6. Intact mass of the Ag85C-EBS covalent complex treated with dithiothreitol. The lower intensity peak at 32672.0 Da corresponds to the Ag85C-EBS covalent complex while the highest intensity peak at 32397.5 Da corresponds to the complex reduced by dithiothreitol.

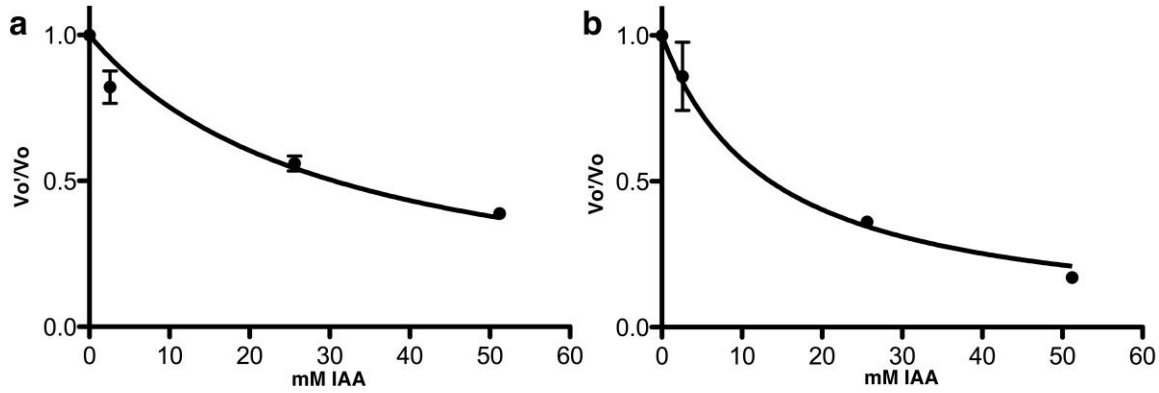

Supplementary Figure S7. Iodoacetamide (IAA) dose-dependence. Error bars (SD) are calculated from triplicate reactions. (**a**) IAA dose-dependence after one hour of incubation with Ag85C. (**b**) IAA dose-dependence after overnight incubation with Ag85C.

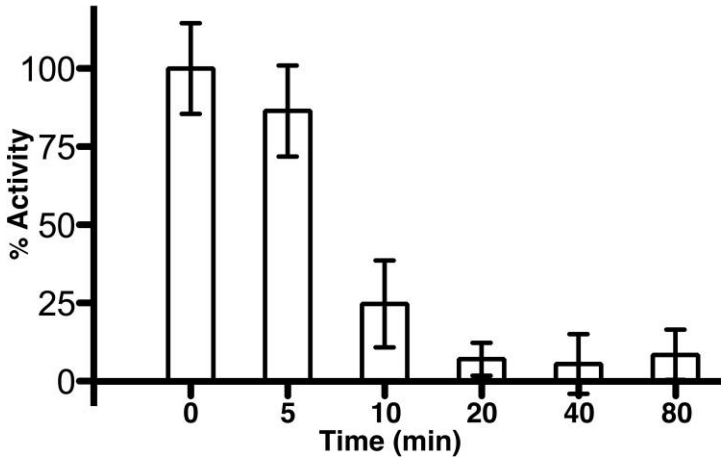

Supplementary Figure S8. Time course of EBS (5 μM) inhibiting Ag85C. Activity is normalized to wild type Ag85C (0 min) and errors bars (SD) are the result of triplicate reactions. The complex Ag85C-EBS was incubated between 5 min and 80 min and was assayed using the resorufin butyrate assay.

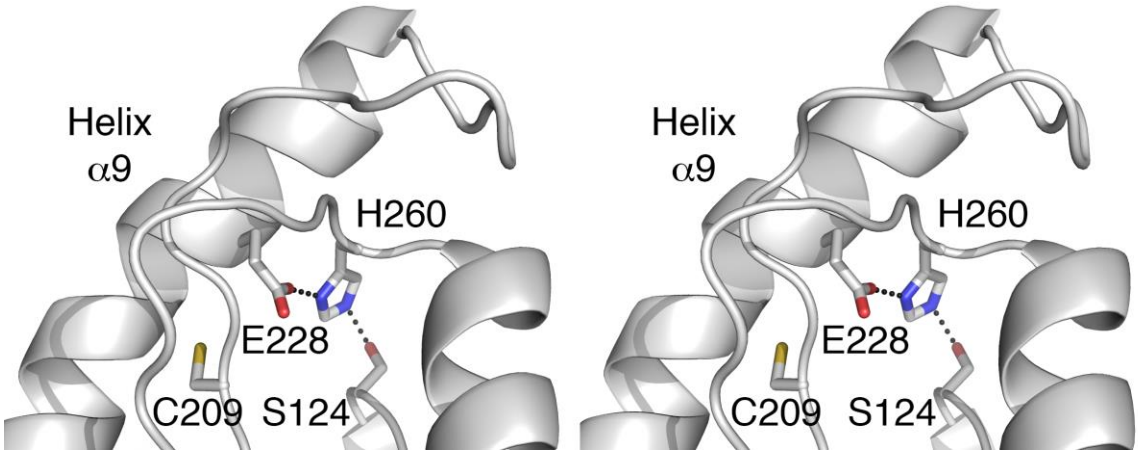

Supplementary Figure S9. Stereo image of native Ag85C active site structure. The backbone cartoon represents the native structure of Ag85C. The residues of the catalytic triad and C209 are colored by CPK. While the kink in helix 9 does not appear pronounced in this orientation, the hydrogen-bonded network formed between the residues of the catalytic triad is easily observed.

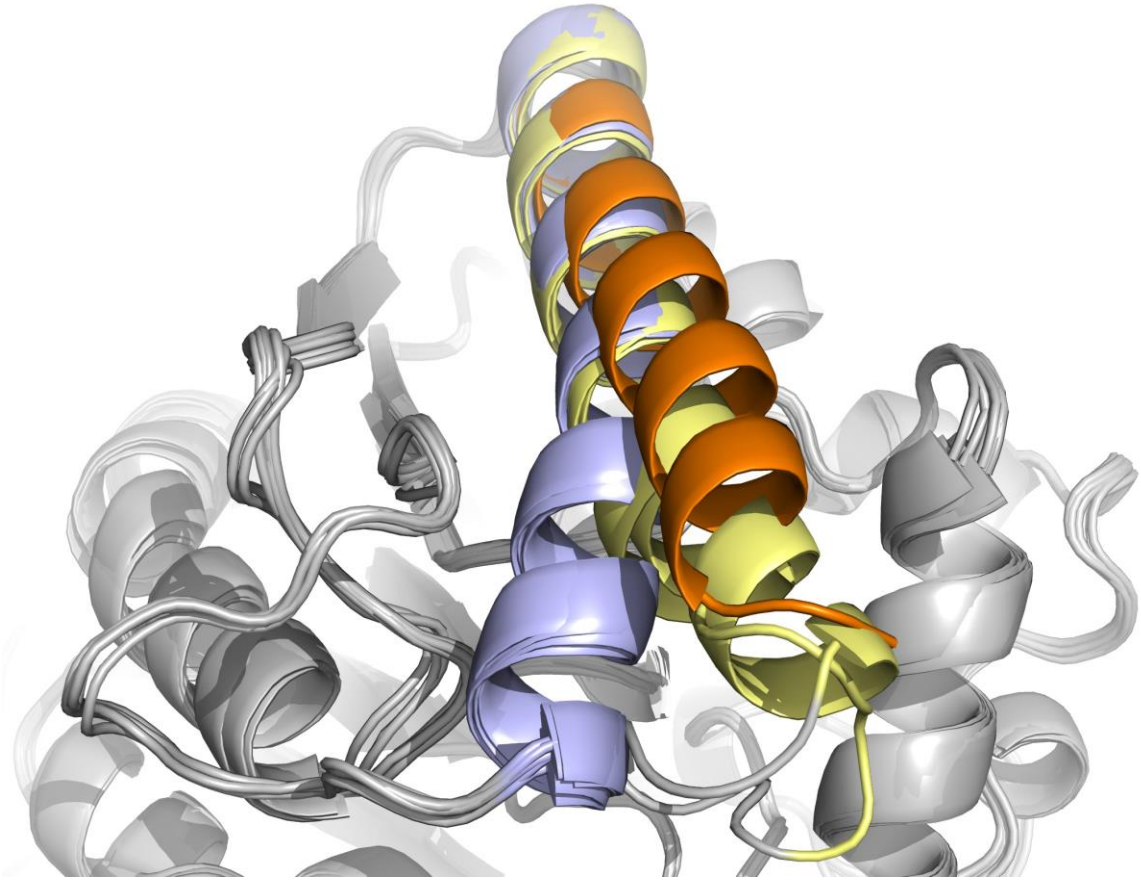

Supplementary Figure S10. Superimposition of several Ag85s: helix α9 of the Ag85 structures in the native form are represented in light blue (Ag85A [1SFR], Ag85B [1F0N], Ag85C [1DQZ], Ag85C-Octylthioglucoside [1VA5], Ag85C-glycerol [3HRH], Ag85C-F1 [37]. Helix α9 of the Ag85C-C209S (PDB accession code 4MQL) mutant and Ag85C-DEP (PDB accession code 1DQY) forms is shown in yellow, and helix α9 of the Ag85C-EBS (PDB accession code 4MQM) structure is shown in orange.

Supplementary Table S1. Peptide mass fingerprinting of Ag85C-2% DMSO control, Ag85C-EBS covalent complex and Ag85C-IAA modified.

Samples	Peptides containing C209	*m*/*z* (calculated)	*m*/*z* (observed)	ΔM
Ag85C	(R)IWVY**C**GNGTPSDLGGDNIPAK(F)	2177.0332	n/o	n/o
	(R)LVANNTRIWVY**C**GNGTPSDLGGDNIPAK(F)	2945.4574	n/o	n/o
	(R)IWVY**C**GNGTPSDLGGDNIPAKFLEGLTLR(T)	3106.5666	3106.5357	0.0309
Ag85C-EBS	(R)IWVY**C**GNGTPSDLGGDNIPAK(F)	2177.0332	2452.1400	275.1068*
	(R)LVANNTRIWVY**C**GNGTPSDLGGDNIPAK(F)	2945.4574	3219.5860	274.1286*
	(R)IWVY**C**GNGTPSDLGGDNIPAKFLEGLTLR(T)	3106.5666	3381.6710	275.1044*
Ag85C-IAA	(R)IWVY**C**GNGTPSDLGGDNIPAK(F)	2177.0332	2235.1330	58.0998**
	(R)LVANNTRIWVY**C**GNGTPSDLGGDNIPAK(F)	2945.4574	n/o	n/o
	(R)IWVY**C**GNGTPSDLGGDNIPAKFLEGLTLR(T)	3106.5666	n/o	n/o

The *m*/*z* values provided correspond to monoisotopic singly-charged ions. n/o: not observed.

* corresponds to EBS covalently attached to C209 (monoisotopic mass = 274.98)

** corresponds to carbamidomethyl from IAA covalently attached to C209 (monoisotopic mass = 57.02)